Extended Range Six DOF High-Precision Positioner for Wafer Processing

Tiejun Hu and Won-Jong Kim, *Senior Member, IEEE*

***Abstract*—A high-precision positioner using a novel superimposed concentrated field permanent magnet matrix is presented in this paper. It can generate all six-degrees-of-freedom (DOF) motions with only a single moving part. This extended range multi axis positioner is actuated by three planar levitation motors, which are attached on the bottom of the moving part. Three aerostatic bearings are currently used to provide the suspension force for the system against gravity. We designed and implemented digital lead–lag controllers running on a digital signal processor (DSP). To improve the closed-loop dynamic performance in the vertical directions, we implemented a controller in the minor feedback loop as well. The positioner demonstrates a position resolution of 20 nm and a position noise of 10-nm root mean square (rms) in x and y and 15-nm rms in z. The angular resolution around the x-, y-, and z-axes is of submicroradian order. The planar travel range is 160 mm × 160 mm, and the maximum velocity achieved is 0.5 m/s at the 5-m/s^2 acceleration, which can enhance the throughput in wafer processing. Several two-dimensional motion profiles are presented to demonstrate the positioner's capability of accurately tracking any extended range planar trajectories. The experimental results verified the utility of this extended range six-DOF high-precision positioner in semiconductor manufacturing and factory automation.**

***Index Terms*—Multi dimensional positioner, precision motion control, real-time digital control, semiconductor manufacturing.**

I. Introduction

THE chip industry is now experiencing a significant PC-driven to consumer-driven transformation, and large, fast-growing consumer markets will have expanding demands for the semiconductor devices. As the 65-nm production moves to a high volume and the development activity of the 45-nm node technology is gearing up, how to maximize the production yields of high-quality devices becomes one of the critical problems for the semiconductor manufacturing industry [1]. As a result, the capital equipment manufacturers are expected to supply more high-performance, high-throughput equipment with cutting edge technology than ever. However, current high precision mechanisms used in the wafer stages are usually designed to work with mechanical constraints such as linear guidance and rotary axes [2]. To achieve precision position capability, the requirements and costs to manufacture these mechanisms are fairly high. Due to the Coulomb friction existing in the mechanical contacts, conventional positioning systems cannot have a fast response or multi dimensional positioning capability without auxiliary axes [3]. Therefore, a better actuation methodology that can easily generate the multi dimensional motion with nanometer position resolution is desired for the future wafer-stepper design.

Conventional mechanical stages for x-y positioning typically use the crossed axis-type or gantry-type configurations [4]–[6]. However, planar motors can neatly simplify the designs due to their unique structures for motion control. Planar motors can be mainly categorized as the variable-reluctance type, the permanent matrix type, and the induction type [7]–[12]. Among them, induction planar motors were designed at the laboratory level. The Sawyer motor, which is a type of variable-reluctance planar motor, was commercialized by Northern Magnetics and Megamation, and is usually operated in open loop. According to Northern Magnetics, the two-phase full-step size is as coarse as 250 μm with a possibility of reduction by microstepping. In addition to the large cogging force, the attractive force of one model is as large as 1800 N [13]. Megamation's x-y stage has been used in an IBM printed circuit board assembly line, and its accuracy specification is about 25 μm.[1] A commercialized wafer stepper, PAS 5500/850D DUV, the step-and-scan system of ASML is for 110-nm mass production and has a field size of 26 mm × 33 mm.[2]

The multi dimensional positioner actuated by synchronous permanent magnet planar motors (SPMPMs) presented in this paper, overcomes all the shortcomings of the established Sawyer motor technology and can generate all fine and coarse motions with only one levitated moving part required for the wafer positioning. This prototype achieved a 20-nm closed-loop positioning resolution and 160 mm × 160 mm travel range without requiring an additional primary coarse-motion or secondary fine-motion stage. As three aerostatic bearings are used to levitate the positioner, the heat generated by the planar motors is dramatically reduced, compared to the positioners levitated by magnet forces only. Therefore, this stage has a better thermal stability than those of maglev stages. The positioner employs a novel superimposed concentrated field double-axis magnet matrix [14] to improve the positioner's force capability. Its cogging force is less than a fraction of 1 N without a strong attractive force.

This positioning technology has the potential to satisfy the dynamic performance specifications necessary for next-generation deep-submicrometer semiconductor manufacturing equipment with significant advantages.

Manuscript received June 25, 2004; revised January 1, 2006. Recommended by Technical Editor I.-M. Chen. This work was supported by Texas Advanced Technology Program under Grant 000512-0225-2001.

T. Hu is with Hysitron Incorporated, Minneapolis, MN 55344-2221 USA (e-mail: hu_tie_jun@hotmail.com).

W.-J. Kim is with the Department of Mechanical Engineering, Texas A&M University, College Station, TX 77843-3123 USA (e-mail: wjkim@tamu.edu).

Digital Object Identifier 10.1109/TMECH.2006.886224

[1] Megamation, http://www.megamation.com/hm_frame.htm, 2001.

[2] ASML, http://www.asml.com/asmldotcom/show.do?ctx=6677&rid=6687, 2006.

1083-4435/$20.00 © 2006 IEEE

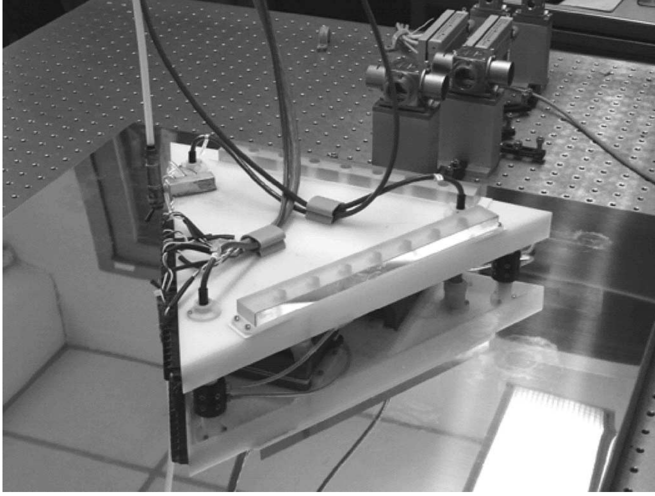

Fig. 1. Photograph of the multi DOF positioner. Triangular platen is placed on top of a mirror-finished aluminum plate, and beneath the aluminum plate is the superimposed concentrated field magnet matrix [15].

1) A noncontact stage requires no lubricants, does not generate wear particles, is noncontaminating, and thus, is highly suited for clean-room environment.
2) Footprint is reduced by superimposing the multiple linear motors into one unified actuation system.
3) One moving part can be designed to have high natural frequencies compared with the prevailing multi element stages with complex dynamics.
4) By eliminating complicated mechanical elements, the fabrication cost is reduced and the reliability is increased.

Therefore, the development of the extended range six-DOF high-precision motion generation technology holds promise for future semiconductor manufacturing and factory automation applications.

The positioner's detailed mechanical design and construction was described in our previous publication [15]. In this paper, dynamic analysis, system modeling, and controller design are discussed in Section III. Key experimental results are presented in Section IV to demonstrate the applicability of this positioner in semiconductor manufacturing. Section V concludes this paper.

II. The Six-DOF Positioner for Wafer Processing

Fig. 1 shows a photograph of the fabricated multi DOF positioning system. The single-moving platen of this positioner is levitated by three aerostatic bearings. Since it will generate no wear particles, it is highly suited for the clean-room environment. Furthermore, this six-DOF positioner provides a unique combination of long-travel range and high-precision position resolution with no additional complicated mechanism.

A. Superimposed Concentrated Field Magnet Matrix

In the magnet arrays used for conventional linear permanent magnet motors, there exists a two-sided magnetic field if no iron backing is used. In the typical cases with the winding on only one side of the array, half of the field is wasted. A type of magnet arrays that provides a magnetic field concentrated to one side of the array was first proposed by Halbach for use in undulators and particle accelerators [16]. Marinescu and Marinescu also studied such a magnet array in [17], where it is represented by a two-dimensional (2-D) multipole field expansion via a complex variable theory. Abele *et al.* represented the magnet array in spherical harmonics and calculated its coefficients [18]. Leupold *et al.* suggested a free-electron laser with a pair of permanent magnet wigglers with a Halbach array [19]. The Halbach magnet array has the remarkable property of primarily single-sided field pattern, which can be seen from the flux lines of a square Halbach magnet array presented in [20]. The superimposed concentrated field magnet matrix beneath the shining aluminum plate, as shown in Fig. 1, is manufactured by a linear superimposition of two orthogonal Halbach magnet arrays [15]. The 2-D magnet matrix's field lines are their orthogonal superimposition, and a detailed study can be found in [21].

B. Moving Platen Design

There are two different ways to design this positioning system, namely, the moving magnets stationary windings design and the moving windings stationary magnets design. Therefore, the moving platen can be designed to carry either the magnets or the windings. Among the two design concepts, we decided on the moving windings design to avoid excessive power consumptions in the inactive winding area coils. Furthermore, we can attain the six-DOF motion generation capability with only three independent levitation motors as shown in Fig. 2. Each levitation motor in Fig. 2 can generate a horizontal as well as a vertical force [22]. Two stick mirrors are mounted on the top of the platen for the three-axis laser interferometry for the horizontal position feedback. The position information in the other three DOFs was obtained using three laser distance sensors.

Fig. 3 presents an assembly process of the three sets of windings. Three Delrin cores without iron are designed to attach the windings to the bottom of the platen, so the magnetic attractive force between the platen and the stationary magnet matrix is negligible. Twelve coils are stacked together side by side to become a three-phase, two-pitch levitation motor mover by soldering the inner leads from inside and the outer leads from outside for every two coils.

Three laser distance sensors 1, 2, and 3 are employed for the vertical position feedback as shown in Fig. 4. A cartesian coordinate system *xoy* is attached on the platen with the origin o at the platen mass center, where $z_{x(1,2,3)}$ and $z_{y(1,2,3)}$ denote the distances of each sensor to the y- and x-axis, respectively. The relation between the readings z_1, z_2, and z_3 of each sensor and the vertical position θ, ψ, and z can be derived as (1). Therefore, the vertical displacement vector can be calculated by multiplying the inverse or the coefficient matrix in (1) and the vector representing sensor's readings

$$\begin{bmatrix} z_1 \\ z_2 \\ z_3 \end{bmatrix} = \begin{bmatrix} -z_{y1} & -z_{x1} & 1 \\ z_{y2} & -z_{x2} & 1 \\ -z_{y3} & z_{x3} & 1 \end{bmatrix} \begin{bmatrix} \theta \\ \psi \\ z \end{bmatrix}. \tag{1}$$

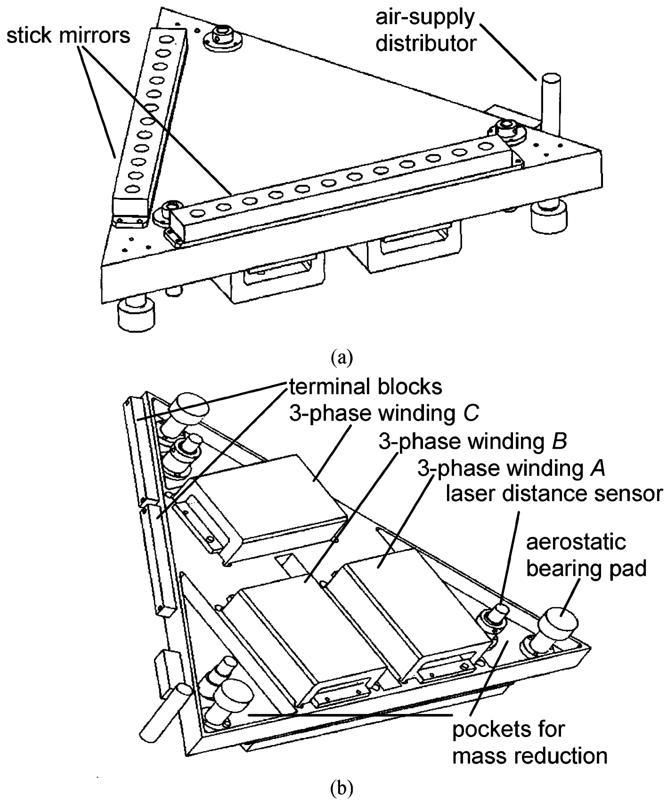

Fig. 2. Perspective views of the levitated platen. (a) Top view. (b) Bottom view. The length of the sides of the triangular platen is 381 mm. The platen carries two stick mirrors for the horizontal metrology and three laser proximity sensors for the vertical metrology. It carries three sets of independent three-phase windings (*A*, *B*, and *C*) that can generate vertical and horizontal forces and avoid the over-constraint issue with four sets of windings.

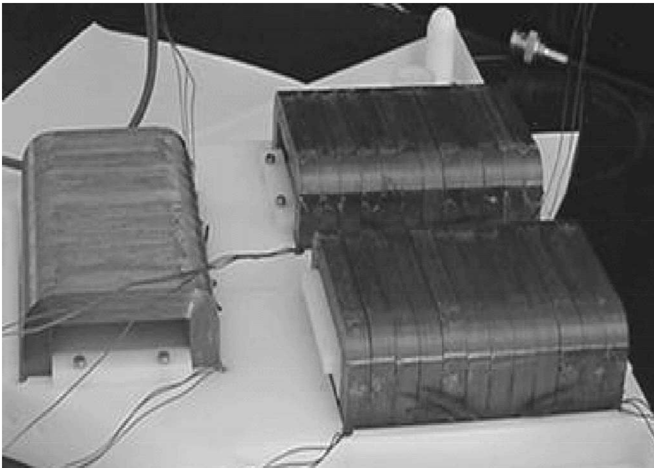

Fig. 3. Assembly process of the planar-motor windings.

With a triangular arrangement of such levitation motors, as shown in Fig. 5, the platen can generate all the six-axis motions for focusing and alignment, and large 2-D step-and-scan motions for high-precision positioning as a wafer stage in semiconductor manufacturing.

For example, we activate positive $F_{\mathrm{A}y}$ and $F_{\mathrm{B}y}$ in Fig. 5 to generate a translational motion in the positive y direction. If $F_{\mathrm{A}y}$ and $F_{\mathrm{B}y}$ are in opposite directions, we get a rotational motion around the z-axis. The translation in the x direction was generated by the force $F_{\mathrm{C}x}$ of motor C with an error torque cancellation by $F_{\mathrm{A}y}$ and $F_{\mathrm{B}y}$. To generate a positive rotation around the x-axis, the platen is driven with a positive $F_{\mathrm{C}z}$ and a negative $F_{\mathrm{A}z}$ and $F_{\mathrm{B}z}$. Motions in the other two DOFs are generated likewise. The asymmetry of the motor arrangement can cause parasitic motions. To minimize this parasitic motion, we implemented an error-torque compensation routine in a real-time C code [23].

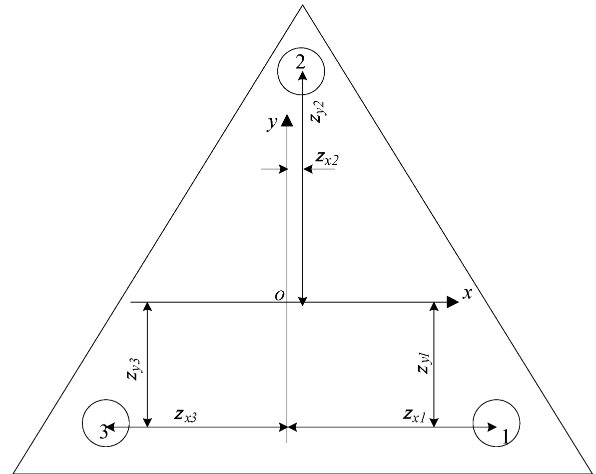

Fig. 4. Top view of laser distance sensors.

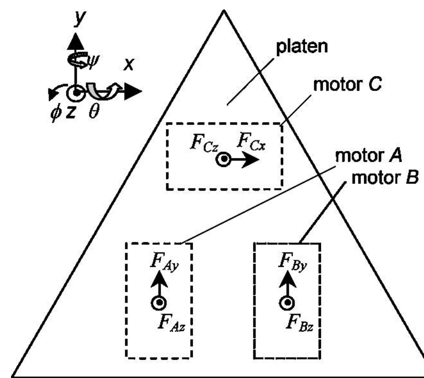

Fig. 5. Definition of the individual force components generated by levitation motors *A*, *B*, and *C* as well as the coordinate axes.

III. Dynamic Modeling and Control System Design

A. Dynamics Modeling

We developed a theoretical framework to determine the resulting force generated by a levitation motor [20]. The size of each winding, set in Fig. 2(b), is 45.78 mm $\times$ 72.59 mm $\times$ 101.95 mm, the actuator pitch is $l = 50.8$ mm, and the air gap between the magnet matrix and the windings is $z_0 = 2.324$ mm. The magnet matrix thickness is $\Delta = l/4$ and the winding thickness is $\Gamma = l/5$, determined via a power optimal design [22]. With these parameters, we calculate the driving force for this positioner of 22.87 N with 2×10^6 A/m^2 peak current density [15]. This is a sufficient force to accelerate the platen mass of 5.91 kg at 1/2 g (5 m/s^2).

The mass of the platen was measured with a precision balance as 5.91 kg, and the calculated inertia matrix in kg·m^2, taken at the platen center of mass, was

$$I = \begin{bmatrix} I_{xx} & -I_{xy} & -I_{xz} \\ -I_{yx} & I_{yy} & -I_{yz} \\ -I_{zx} & -I_{zy} & I_{zz} \end{bmatrix} = \begin{bmatrix} 0.0357 & -0.00120 & -0.000808 \\ -0.00120 & 0.0261 & 0.000263 \\ -0.000808 & 0.000263 & 0.0561 \end{bmatrix}. \quad (2)$$

As the products of inertia are less than 5% of the principal moments of inertia, we neglect them in the present dynamic model.

Although the three levitation motors were sized to be able to levitate the platen magnetically, we use three aerostatic bearings to provide the suspension force against the gravity to reduce the power consumption in the system. As a result, the platen is modeled as a pure mass without friction for the translation in the x and y directions. The dynamics of this pure mass model is presented by the Newton's equation of motion

$$M\frac{d^2x}{dt^2} = f_x \quad (3)$$

$$M\frac{d^2y}{dt^2} = f_y \quad (4)$$

where M is 5.91 kg and $f_{(x,y)}$ is the magnetic modal forces generated by the planar motors.

For the control of rotation around the z-axis, the dynamics of: the system is represented by the following differential equation

$$I_{zz}\frac{d^2\phi}{dt^2} = \tau_z \quad (5)$$

where τ_z is the torque from the magnetic origin about the z-axis and I_{zz} is the principal moment of inertia about the z-axis.

The platen is modeled as a spring-mass system in the z-axis because of the existence of the three aerostatic bearings

$$M\frac{d^2z}{dt^2} + K_z z = f_z \quad (6)$$

where K_z is the effective spring constant of the aerostatic bearings and f_z is the vertical modal force generated by the three motors. By an experiment based on the Hooke's law, K_z was measured as 1.00×10^6 N/m.

As the three aerostatic bearings can be regarded as three springs, the dynamics in the rotation around the x- and y-axes can also be modeled as a spring-mass system

$$I_{xx}\frac{d^2\theta}{dt^2} + K_\theta\theta = \tau_\theta \quad (7)$$

$$I_{yy}\frac{d^2\psi}{dt^2} + K_\psi\psi = \tau_\psi \quad (8)$$

where τ_θ and τ_ψ are the modal torques around the x- and y-axes, respectively, and K_θ and K_ψ are the effective torsional spring constants with regard to the x- and y-axes, which were determined as 1.12×10^4 and 1.17×10^4 N·m/rad by experiments, respectively. Refer to [23] for a full six-DOF state-space model for the combined six-DOF motions.

B. Horizontal Motion Control

A Pentek 4284 board with a TMS320C40 DSP is used to perform the real-time digital control of the system. A versa module eurocard (VME) personal computer is used to compile the C codes and load the executable file to the DSP. Three laser interferometers and laser-axis boards (Agilent 10897B) with a resolution of 0.6 nm are used to obtain the three-DOF position information (translations in x and y as well as the rotation around z) in the horizontal plane. These digital sensor signals are directly sent to the DSP. In the vertical directions, three laser distance sensors (Nanogage 100) are employed for the vertical position (translation in z as well as the rotations around x and y) feedback. These sensors pass the vertical-axis position measurements to the 16-bit analog-to-digital converters (ADCs), which communicate with the DSP via the MIX bus through first-order *RC* anti-aliasing filers with a cut-off frequency of 1 kHz.

An interrupt service routine (ISR), which we developed, processes all the position measurement data and computes the control outputs for the positioner, and runs on the DSP at the sampling frequency of 5 kHz [23]. Once the control outputs are calculated, they are sent to a nine-channel power amplifier through the 12-bit digital-to-analog converters (DACs). Then, this amplifier passes the commanded nine independent phase currents through the levitation motor winding sets to generate the actuation forces.

The second-order digital lead–lag controllers were designed for the translation motions in the x- and y-axis. The implemented digital lead–lag compensator is

$$G_{x,y}(z) = 740000\left(\frac{z-0.9903}{z-0.7970}\right)\left(\frac{z-0.9979}{z-1}\right). \quad (9)$$

The crossover frequency of this control system is 21 Hz, and the phase margin is 57.6°. A similar digital lead–lag controller is designed to control the rotation around the z-axis as follows:

$$G_\phi(z) = 13100\left(\frac{z-0.9903}{z-0.7970}\right)\left(\frac{z-0.9979}{z-1}\right). \quad (10)$$

Here, the crossover frequency is 38 Hz, and the phase margin is 62.7°.

C. Vertical Motion Control

In the vertical dynamics, there exists a resonance due to the aerostatic bearing springs in the system. For the z-, θ-, and ψ-axis, the resonance frequencies are 65.5, 89.2, and 107 Hz, respectively. This resonance degrades the dynamic performance of the system significantly and may cause system instablility. To improve the dynamic performance in the vertical axes, we designed an inner-loop controller based on the following feedback structure.

The controller $C(s)$ is implemented in the feedback path to mitigate the effect of the aerostatic bearing resonance in the vertical dynamics. It modifies the original plant so that the overall closed loop can have a more stability margin and a faster step response. The resonance peak was significantly reduced after the controller $C(s)$ was implemented in the minor loop. The implemented digital controllers $C(z)$ in all the three vertical

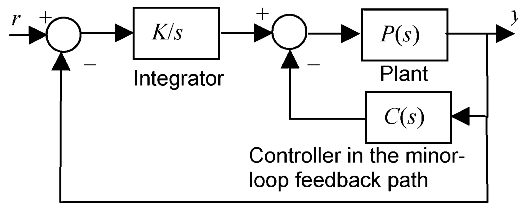

Fig. 6. Control structure in the vertical direction control.

axes are

$$C_z(z) = 3.000 \times 10^6 \frac{z-1}{z-0.8187} \tag{11}$$

$$C_{\theta,\psi}(z) = 1.083 \times 10^4 \frac{z-1}{z-0.8465}. \tag{12}$$

Then we added an integrator K/s in the outer loop to eliminate the steady-state position error. The values of K for z, θ, and ψ are 10 000 N/m·s, 100 N/rad·s and 100 N/rad·s, respectively. The phase margin of the entire control system, as shown in Fig. 6, now became as much as 87.1° in the ψ-axis.

IV. Experimental Results

For a wafer stage to satisfy the requirements of semiconductor manufacturing, the positioner should have a nanoscale positioning resolution, fast response, and an extended travel range. In addition, the capability of generating any 2-D trajectory is also necessary for such a positioner to be used in the wafer inspection process. The multi DOF positioner, presented herein, has the potential to satisfy all these requirements. Several experimental results are presented in this section to demonstrate its applicability in future semiconductor manufacturing and factory automation.

A. Micro- and Nanoscale Multi DOF Positioning

To test the dynamic performance of the positioning system, we obtained its step responses in all the six axes, as shown in Fig. 7. The rise time is less than 3 ms, and the settling time is less than 150 ms without the steady-state error in the x and y directions. The overshoot is less than 20% [Fig. 7(a) and (b)]. The rise time of the vertical step responses [Fig. 7(c), (d), and (e)] is a little longer than that in the horizontal ones, because of the compensated aerostatic bearing dynamics and the lower bandwidth of the controllers in the vertical axes. However, it can be noticed that there is no overshoot in the vertical step responses, which is important to reduce the vibration and prevent any unwanted disturbance in wafer processing. The low-frequency (at about 10 Hz) disturbance in ϕ is believed to be generated by the umbilical cables and air pipes connected to the moving platen.

Fig. 8(a) and (b) presents the 30-nm step responses in x and y, Fig. 8(c) the 1-μm step response in z, and Fig. 8(d), (e), and (f) the 1-μrad step responses in θ, ψ, and ϕ, respectively. There exists a 10-nm-rms position noise in the system. The position noise might originate from the measuring noise of the laser interferometer and laser distance sensor, D/A A/D quantization noise, electrical noise of power amplifier and the external disturbances

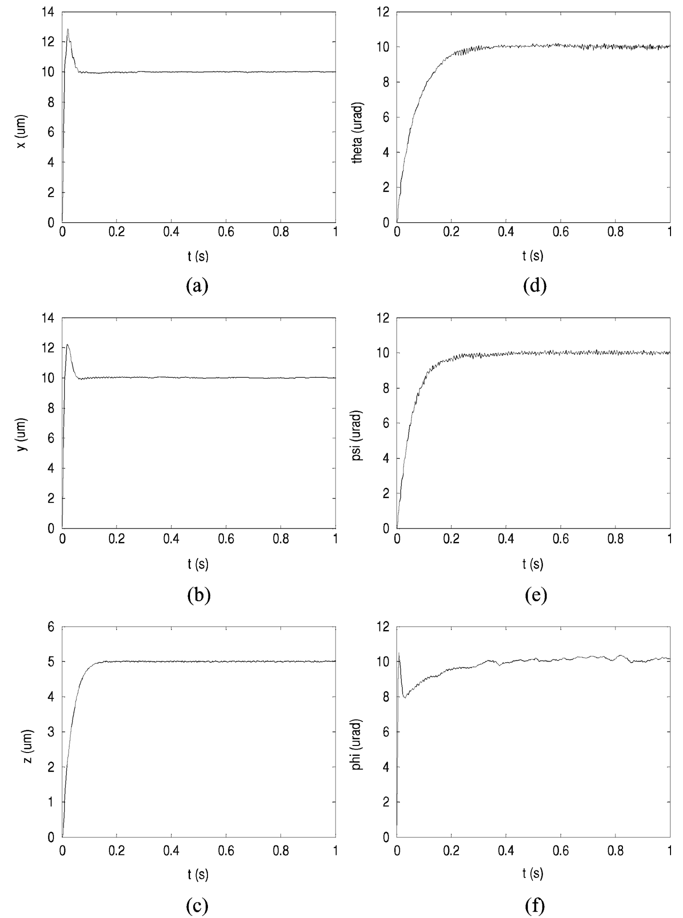

Fig. 7. 10-μm step responses in (a) x and (b) y. (c) 5-μm step response in z. 10-μrad step responses in (d) θ, (e) ψ, and (f) ϕ.

from optical table, aerostatic bearings, and the umbilical cables. Assuming all the noise and disturbances are white Gaussian noise, we can obtain the noise/disturbance propagation model for our system [24]. With the resolution of the sensors, quantization errors of the D/A converter, and dynamics of the system as well as the experimentally measured disturbance data obtained by accelerometers, we can theoretically calculate the position noise in the horizontal plane is 8-nm rms, which matched fairly well with the real noise, existing in Fig. 8. These experimental results demonstrate the nanometer-precision positioning capability of the positioner.

B. Microscale Sinusoidal and Circular Motion Generation

Figs. 9 and 10 show that the positioner can precisely follow any microscale trajectory in the x-y plane. Figs. 9(b) and 10(b) indicate that the position noise in following the commanded trajectories is less than 30-nm rms. It is likely that the pneumatic hammer causes this pitching noise, and we get Abbe error due to the mismatch between the platen mass center and the sensor locations. However, these experimental results demonstrate the positioner's capability of one-dimensional (1-D) and 2-D precision positioning.

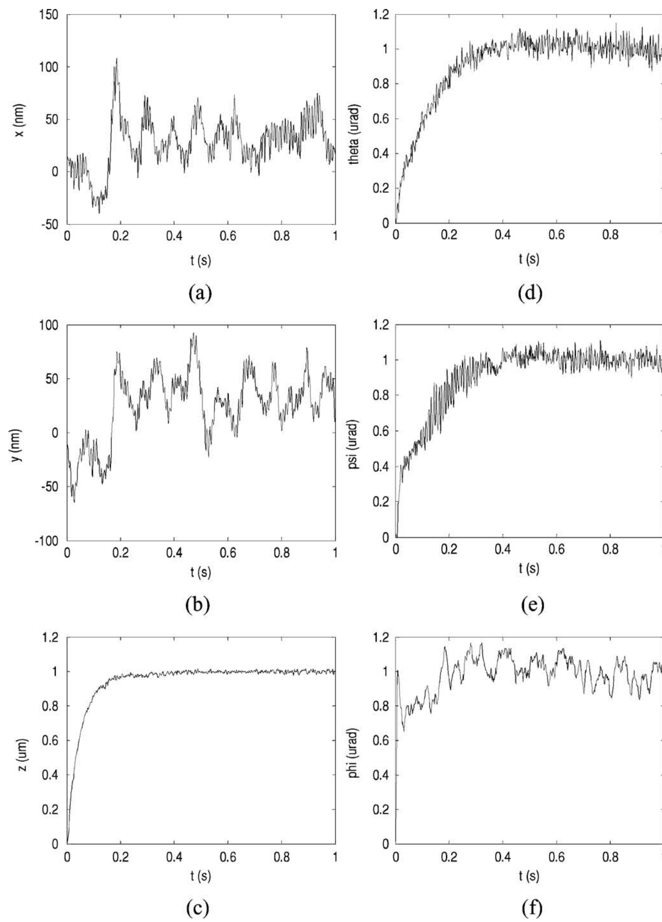

Fig. 8. 30-nm step responses in (a) x and (b) y. (c) 1-μm step response in z. 1-μrad step responses in (d) θ, (e) ψ, and (f) ϕ.

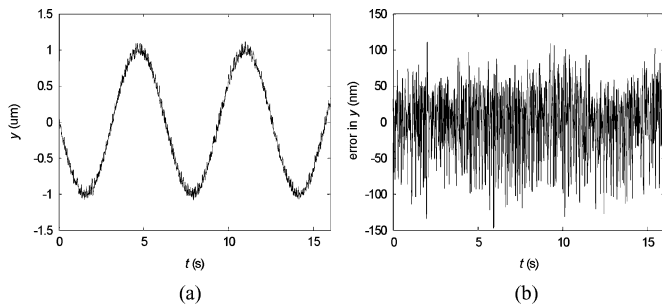

Fig. 9. (a) 1-μm amplitude sinusoidal motion. (b) Error with respect to the commanded trajectory in y.

C. Fast Motion for High Throughput

The six-DOF positioner is currently capable of generating the maximum velocity of 0.5 m/s with the maximum acceleration of 5 m/s^2 in the y direction. Fig. 11(a) shows the stage moved back and forth with a range of 140 mm in y. The platen first moved in the positive y direction at the maximum acceleration of about 0.5g (5 m/s^2). When the velocity reached 0.5 m/s, the platen stopped accelerating and moved at this constant velocity. After 0.18 s, the platen started to decelerate at 5 m/s^2 until its velocity reached zero. After resting at the position of 140 mm for a while, the stage moved back to its original position in the same way as it moved forth. Fig. 11(b) shows the corresponding velocity profile. A 10% overshoot in the velocity is visible at the end of abrupt velocity changes. The 0.5 m/s maximum velocity is limited by the laser interferometry, which we employ and not by our technology.

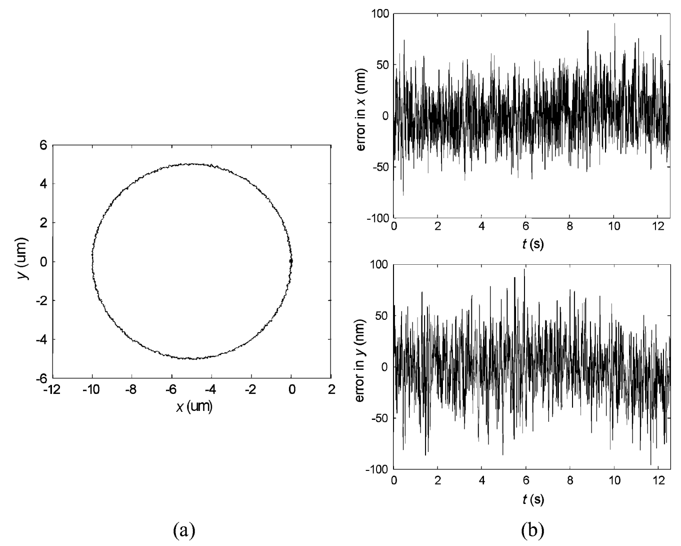

Fig. 10. (a) 5-μm radius circle in the x-y plane. (b) Positioning error in x and y, respectively. The positioner completed this circular trajectory in 12.56 s at a constant angular velocity of 0.5 rad/s.

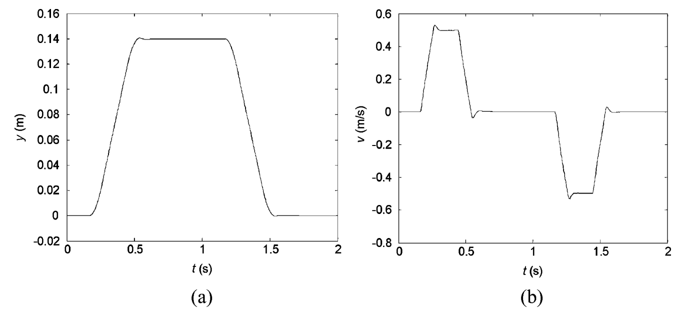

Fig. 11. Profiles in y with the 0.5-m/s maximum velocity and 5-m/s^2 maximum acceleration. (a) Position. (b) Velocity.

To generate an acceleration of 5 m/s^2 in the y direction, as shown in Fig. 11, the corresponding force, the two planar motors A and B should provide, is 29.6 N. Therefore, the nominal three-phase currents in one motor can be calculated as 0.733, 0.367, and -0.367 A, respectively. With a 19.4-Ω winding resistance, the maximum thermal power generated by one motor can be calculated as 15.7 W. Since the acceleration/deceleration time is only 0.1 s, the heat generated by one motor is 1.57 J. The average of the steady-state power consumptions of all the three motors can be determined to be 12.6 mW by experimentally recording the instant currents in each motor while the platen is in the steady state.

D. Step-and-Repeat Motion for Stepper Application

In the photolithographic process of chip fabrication, a wafer stage would carry a silicon wafer (200 or 300 mm in diameter) from one die sit to another to repeat the exposure to the laser.

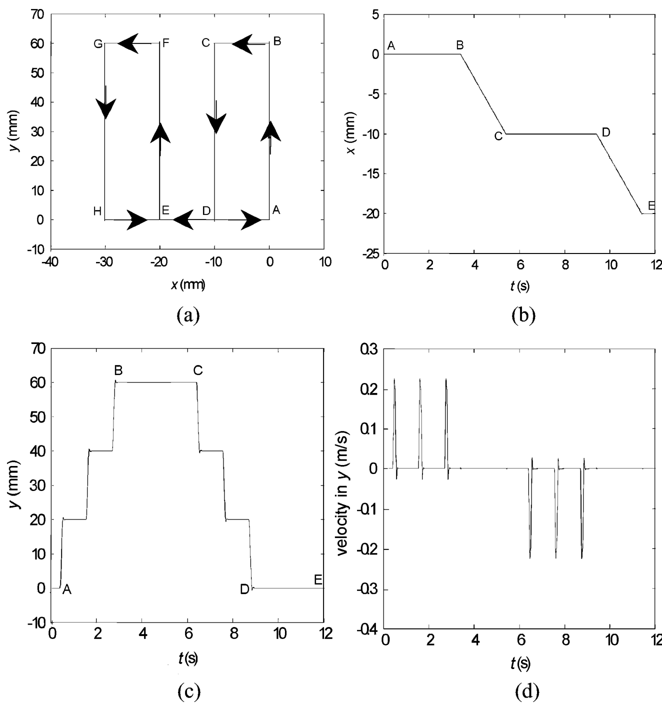

Fig. 12. (a) Experimental motion profile of a 2-cm step-and-repeat motion in the y direction traversed by the platen. Position trajectory in (b) x direction and (c) y direction. (d) Velocity profile in the y direction.

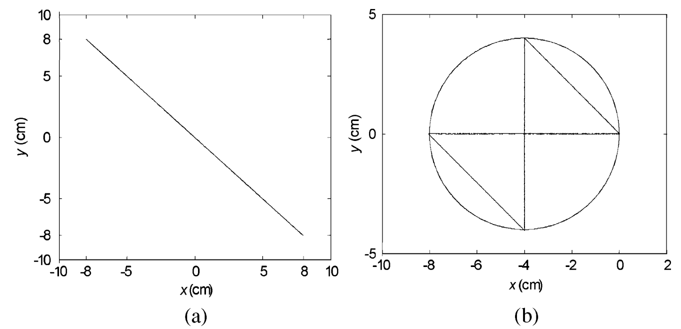

Fig. 13. (a) Actual 160 mm $\times$ 160 mm planar travel range in the x-y plane traversed by the platen. (b) Actual 4-cm radius circle combined with a double triangle trajectory traversed by the platen.

These step-and-repeat steppers have dominated in IC fabrication since late 1980s [25]. The positioner herein can simulate the similar step-and-repeat motion, which is used in semiconductor manufacturing. Fig. 12 presents a sample step-and-repeat motion profile both in the position and velocity. Here, 2 cm was chosen as a typical die size.

The positioner started from point A at the origin of its coordinate system with an acceleration of 4 m/s^2 in the positive y direction. After its velocity reached 0.2 m/s, it moved for 50 ms at this velocity. Then, it decelerated at an acceleration of -4 m/s^2. After 50 ms, the velocity was reduced to 0 m/s. Then, one 2-cm step was completed. This 2-cm step was repeated three times in the positive y direction until the positioner reached point B. Then, the positioner moved with a constant velocity of -5 mm/s [as seen in Fig. 12(b)] in the x direction until it reached the point C. After that, the positioner moved back from C to D in the same way as that from A to B, yet in the opposite direction. The same motion was repeated in the rest of the trajectory from D to H. When the positioner reached point H, it began to move back to the origin point A in the x direction. In Fig. 12(b), (c) and (d), we present the experimental results for the first 12 s to enhance the resolution of the subplots. The rest of the trajectories are similar.

E. Large Planar Motion Generation

Fig. 13(a) shows that the positioner has a travel range of 160 mm both in the x and y directions. The positioner traversed the whole range with a constant velocity of 5 mm/s both in x and y. Fig. 13(b) demonstrates that the positioner has the capability of following both the curved and straight-line long-range trajectories in the x-y plane. The angular velocity was 0.5 rad/s in the circle and the linear velocity was 5 mm/s in the double triangle. These experimental results, as shown in Fig. 13, verify that the stage has an extended travel range and that it can generate any planar motion in the x-y plane.

V. Conclusion

An extended range six-DOF high-precision positioning system consisting of a novel superimposed concentrated field double-axis magnet matrix with a triangular single-moving platen was developed and tested. The actuators for the positioner are three three-phase linear levitation motors. Each of these motors can generate vertical as well as lateral forces. The mass of the single-moving triangular platen is only 5.91 kg.

The digital lead–lag compensators were designed to control the horizontal motions. By implementing a controller in a minor feedback loop, we successfully eliminated the aerostatic bearing resonance in the vertical axes. After implementing these digital feedback controllers, we achieved a position resolution of 20 nm with a position noise of 10-nm rms in both x and y, and a submicrometer resolution in the other axes. The positioning error in tracking a 1-μm sinusoidal wave and a 5-μm radius circle was less than 30-nm rms, which demonstrated the positioner's 1-D and 2-D nanoscale positioning capabilities.

Several experiments were performed to evaluate the potential application of this positioner in semiconductor manufacturing. The 2-cm step-and-repeat motion with an acceleration of 4 m/s^2 generated by the positioner indicates that it has the potential to be used as a wafer stepper in semiconductor factory automation.

This prototype positioner has a planar travel range of 160 mm $\times$ 160 mm, which can be easily extended by adding more magnets to the magnet matrix. It currently has 0.5-m/s maximum speed at an acceleration of 5 m/s^2. The large arbitrary planar-motion generation capability of this positioning stage was demonstrated by following large 2-D motion profiles such as a 4-cm-radius circle combined with a double triangle. These extended range tracking capabilities make this prototype positioner qualified to be used as a wafer inspection stage. We demonstrated experimentally that the extended range six-DOF positioner, presented in this paper, was suitable for the semiconductor manufacturing and factory automation applications.

REFERENCES

[1] M. G. Pum and D. Dutton, "Executive roundup: What 2006 has in store," *Semicond. Int.*, vol. 29, no. 1, pp. 52–62, Jan. 2006.

[2] X. Shan, S.-K. Kuo, J. Zhang, and C.-H. Menq, "Ultra precision motion control of a multiple degrees of freedom magnetic suspension stage," *IEEE/ASME Trans. Mechatronics*, vol. 7, no. 1, pp. 67–78, Mar. 2002.

[3] K. S. Jung and Y. S. Baek, "Precision stage using a non-contact planar actuator based on magnetic suspension technology," *Mechatronics*, vol. 13, no. 8, pp. 981–999, Oct. 2003.

[4] Maricopa Advanced Technology Education Center, *Semiconductor Manufacturing Technician Skill Standards*. Tempe, AZ: Maricopa Community College District, 2000.

[5] G. Van Engelen and A. G. Bouwer, "Two-step positioning device using Lorentz forces and a static gas bearing," U.S. Patent 5 120 034, Jun. 1992.

[6] S. Sakino, E. Osanai, M. Negishi, M. Horikoshi, M. Inoue, and K. Ono, "Movement guiding mechanism," U.S. Patent 5 040 431, Aug. 1991.

[7] J. Cao, Y. Zhu, J. Wang, W. Yin, and G. Duan, "Analysis and comparison of two-dimensional permanent-magnet arrays for planar motor," *IEEE Trans. Magn.*, vol. 40, no. 6, pp. 3490–3494, Nov. 2004.

[8] H.-S. Cho, C.-H. Im, and H.-K. Jung, "Magnetic field analysis of 2-D permanent magnet array for planar motor," *IEEE Trans. Magn.*, vol. 37, no. 5, pp. 3762–3766, Sep. 2001.

[9] H.-S. Cho and H.-K. Jung, "Analysis and design of synchronous permanent-magnet planar motors," *IEEE Trans. Energy Convers.*, vol. 17, no. 4, pp. 492–499, Dec. 2002.

[10] N. Fujii and T. Kihara, "Surface induction motor for two-dimensional drive," *Trans. Inst. Electr. Eng. Jpn.*, vol. 118, no. 2, pp. 221–228, Feb. 1998.

[11] T. Asakawa, "Two-dimensional positioning devices," U.S. Patent 4 626 749, Dec. 1986.

[12] A. Chitayat, "Two-axis motor with high density magnetic platen," U.S. Patent 5 777 402, Jul. 1998.

[13] *Northern Magnetics Linear Motor Technology Manual*, Normag, Santa Clarita, CA, 1998.

[14] D. L. Trumper, W.-J. Kim, and M. E. Williams, "Magnetic arrays," U.S. Patent 5 631 618, May 1997.

[15] W.-J. Kim, N. Bhat, and T. Hu, "Integrated multidimensional positioner for precision manufacturing," *Proc. Inst. Mech. Eng. Part B J. Eng. Manuf.*, vol. 218, no. 4, pp. 431–442, Apr. 2004.

[16] K. Halbach, "Design of permanent multipole magnets with oriented rare earth cobalt material," *Nucl. Instrum. Methods*, vol. 169, no. 1, pp. 1–10, Feb. 1980.

[17] M. Marinescu and N. Marinescu, "New concept of permanent magnet excitation for electrical machines. Analytical and numerical computation," *IEEE Trans. Magn.*, vol. 28, no. 2, pp. 1390–1393, Mar. 1992.

[18] M. G. Abele, H. Rusinek, and F. Bertora, "Field computation in permanent magnets," *IEEE Trans. Magn.*, vol. 28, no. 1, pp. 931–934, Jan. 1992.

[19] H. A. Leupold, E. Potenziani, and M. G. Abelle, "Novel magnet structure for free-electron lasers," *J. Appl. Phys.*, vol. 67, no. 9, pp. 4653–4655, May 1990.

[20] W.-J. Kim, "High-precision planar magnetic levitation" Ph.D. dissertation, MIT, Cambridge, Jun. 1997.

[21] Y. Kawato, "Multi-DOF precision positioning methodology using hall-effect sensors" M.S. thesis, Texas A&M Univ., College Station, May 2005.

[22] D. L. Trumper, W.-J. Kim, and M. E. Williams, "Design and analysis framework for permanent-magnet machines," *IEEE Trans. Ind. Appl.*, vol. 32, no. 2, pp. 371–379, Mar./Apr. 1996.

[23] T. Hu, "Design and control of a 6-degree-of-freedom levitated positioner with high precision" Ph.D. dissertation, Texas A&M Univ., College Station, May 2005.

[24] J. Gu, "Development of a 6-degree-of-freedom magnetically levitated instrument with nanometer precision" M.S. thesis, Texas A&M Univ., College Station, May 2003.

[25] M. Quirk and J. Serda, *Semiconductor Manufacturing Technology*. Englewood Cliffs, NJ: Prentice-Hall, 2001.

Tiejun Hu received the B.S. degree in mechanical engineering and the M.S. degree in material processing engineering from Tsinghua University, Beijing, China, in 1999 and 2002, respectively, and the Ph.D. degree in mechanical engineering from Texas A&M University, College Station, in 2005. His doctoral dissertation project involved design and control of a novel six-DOF levitated stage with high precision. The integrated multi dimensional positioning stage can be used in precision manufacturing and has the potential to satisfy the requirements for next generation wafer FABs in semiconductor manufacturing.

He is currently a Senior Project Engineer with Hysitron, Inc., Minneapolis, MN, where he is engaged in the development of nanomechanical test instruments. His current research interests include design and feedback control of high precision servo mechanism, embedded system design and development, nanoscale engineering and technology, power electronics, and digital signal processing.

Dr. Hu is a member of American Society of Mechanical Engineers (ASME). He is the recipient of the 2005 Professional Engineering Publishing Award for the best paper published in 2004 in *Journal of Engineering Manufacture*.

Won-Jong Kim (S'89–M'97–SM'03) received the B.S. (*summa cum laude*) and M.S. degrees in control and instrumentation engineering from Seoul National University, Seoul, Korea, in 1989 and 1991, respectively, and the Ph.D. degree in electrical engineering and computer science from Massachusetts Institute of Technology (MIT), Cambridge, in 1997.

Since 2000, he has been with the Department of Mechanical Engineering, Texas A&M University (TAMU), College Station, where currently he is an Associate Professor. After the Ph.D. degree, he was with SatCon Technology Corporation, Cambridge, MA, for three years. His current research interests include focus on the analysis, design, and real-time control of mechatronic systems, networked control systems, and nanoscale engineering and technology. He is the holder of three U.S. patents on precision positioning systems.

Dr. Kim is member of Pi Tau Sigma and American Society of Mechanical Engineers (ASME). He is the Chair of the ASME Nanoscale Control Technical Panel and a member of the IEEE Nanotechnology Council. He was the recipient of Korean Institute of Electrical Engineers' Student Paper Contest grand prize in 1988, Samsung Electronics' Humantech Thesis gold prize for his MIT dissertation in 1997, the NASA Space Act Award in 2002, and the 2005 Professional Engineering Publishing Award for the best paper published in 2004 in *Journal of Engineering Manufacture*. He was also a semifinalist of the National Institute of Standards and Technology (NIST)'s Advanced Technology Program competition in 2000. He was appointed a Select Young Faculty Fellow by TAMU College of Engineering and the Texas Engineering Experiment Station twice in 2003 and 2005. He received the BP Teaching Excellence Award by TAMU College of Engineering in 2006.